AGE (2014) 36:9690
DOI 10.1007/s11357-014-9690-8

Clustered granules present in the hippocampus of aged mice result from a degenerative process affecting astrocytes and their surrounding neuropil

Gemma Manich · Itsaso Cabezón · Antoni Camins · Mercè Pallàs · Pawel P. Liberski · Jordi Vilaplana · Carme Pelegrí

Received: 12 April 2014 / Accepted: 13 July 2014 / Published online: 30 July 2014

Abstract Clusters of pathological granular structures appear and progressively increase in number with age in the hippocampus of several mice strains, markedly in the senescence-accelerated mouse prone 8 mice. In the present work, we performed an ultrastructural study of these granules paying special attention to the first stages of their formation, which have not been previously explored. The analysis of the immature granules allowed concluding that granules are not simple accumulations of molecular waste but the result of a degenerative process involving principally astrocytic processes, although nearby neuronal structures can be also affected. The granule generation includes the instability of the plasmatic membranes and the appearance of abnormal membranous structures that form intracellular bubbles or blebs of variable sizes and irregular shapes. These structures and some organelles degenerate producing some membranous fragments, and an assembly process of the resulting fragments generates the dense-core nucleus of the mature granule. Moreover, we found out that the neo-epitope recently described in the mature granules and localised abundantly in the membranous fragments of their dense-core nucleus emerges in the first stages of the granule formation. On the other hand, with this study, we increase the evidences that each cluster of granules is formed by the granules comprised in one astrocyte. A better knowledge of the causes of the granule formation and the function of the neo-epitope will help in both the interpretation of the physiological significance of the granules and their contribution to the degenerating processes in aging brain.

Keywords Aging · Hippocampus · Astrocyte · Granules · Neo-epitope · Periodic acid–Schiff · SAMP8

Jordi Vilaplana and Carme Pelegrí contributed equally to this study.

G. Manich · I. Cabezón · J. Vilaplana · C. Pelegrí (✉)
Departament de Fisiologia, Facultat de Farmàcia, Universitat de Barcelona, Av. Joan XXIII s/n, 08028 Barcelona, Spain
e-mail: carmepelegri@ub.edu

A. Camins · M. Pallàs
Unitat de Farmacologia i Farmacognòsia, Facultat de Farmàcia, Institut de Biomedicina (IBUB), Universitat de Barcelona, Av. Joan XXIII s/n, 08028 Barcelona, Spain

A. Camins · M. Pallàs · J. Vilaplana · C. Pelegrí
Centros de Biomedicina en Red de Enfermedades Neurodegenerativas (CIBERNED), Barcelona, Spain

P. P. Liberski
Department of Molecular Pathology and Neuropathology, Medical University of Lodz, Lodz, Poland

Introduction

Aging in mice, as well as in other species, involves several associated morphological and functional changes that can be considered the result of some abnormal or pathological processes. Among others, pathological granular structures appear and progressively increase in number with age in the hippocampus of several mice strains. The positive reaction to the periodic acid–Schiff stain is their main histochemical feature. The granules, sized up to 3 μm in diameter, appear first in the *stratum*

radiatum of CA1 region, and they progressively extend to other hippocampal regions. They do not usually appear isolated, but they tend to form clusters of about 80 μm in diameter each containing approximately 40–50 granules. These clustered granules have been reported, among others, in the brain of aged C57BL/6 mice (Lamar et al. 1976; Jucker et al. 1992), senescence-accelerated mouse prone 8 (SAMP8) mice (Akiyama et al. 1986), AKR mice (Mitsuno et al. 1999) and ICR-CD1 mice (Del Valle et al. 2010). In SAMP8 mice, which present an accelerated process of aging, the granules appear as early as 3 months of age, earlier than in the other reported mice strains, and the number of clusters and granules increases and spreads faster than in the other strains (Jucker et al. 1994; Del Valle et al. 2010).

Ultrastructural studies revealed that granules have a central core of electron-dense crystalline-like fibrillar deposition generally surrounded by a halo or electron-lucent region. The halo is delimited externally by a plasma membrane which suggests a cellular location, although appears discontinuous in some regions. The central core is round to ovoid in shape, and the membrane-like structures contained in it are haphazardly aggregated and do not resemble any cell organelle. Moreover, organelles cannot be observed in this centre. On the contrary, cytoplasmic organelles like endoplasmic reticulum, polyribosomes, intermediate filaments, multivesicular bodies or mitochondria have been occasionally described in the halo region (Kuo et al. 1996; Robertson et al. 1998; Mitsuno et al. 1999; Doehner et al. 2010; Manich et al. 2014). Although it can be considered that the material stored in the centre of the granules is just an accumulation of molecular waste, the successive ultrastructural changes from the exterior to the interior of the granules suggested to some authors that the pathological process is initiated in the outside of the granules and that the degenerative structures migrate inward (Kuo et al. 1996). It must be pointed out that all ultrastructural studies performed until now are based on the observations of mature granules, and immature granules or granules in the first stages of their formation have never been observed. As early as 1999, Mitsuno and co-workers indicated that in order to clarify whether different cells are involved in granule formation, electron microscope studies of the early phase of granule formation were needed (Mitsuno et al 1999). These observations will allow to precise the mechanisms underlying their formation and to unveil their origin.

Whether the origin of the granules is neuronal or astrocytic has not been clarified yet. A neuronal origin has been suggested based on the presence of synaptic contacts to the plasma membrane (Mitsuno et al. 1999), and it has been assumed from another ultrastructural study that granules are located in abnormal synaptic terminals (Irino et al. 1994). In addition, the description of some neuronal origin components, such as amyloid-β peptides (Robertson et al. 1998; Knuesel et al. 2009; Del Valle et al. 2010), neuronal nuclei protein and tau protein (Manich et al. 2011; Krass et al. 2003) or reelin protein (Knuesel et al. 2009) also suggested a neuronal origin or, at least, some involvement of neurons in their formation. In contrast, a remarkably tight relationship between granules and astrocytes has been found in several occasions. In electron microscopy studies, granules have been observed within both the cell bodies and processes of protoplasmic astrocytes that were expanded and their normal content of cytoplasmic organelles greatly diluted (Robertson et al. 1998). Light microscopy and confocal laser microscopy observations revealed that some granules are associated with the processes of glial fibrillary acidic protein (GFAP)-positive astrocytes (Akiyama et al. 1986; Jucker et al. 1994; Manich et al. 2011), and in some cases, a cluster can be directly associated with a GFAP-positive astrocyte (Jucker et al. 1994; Manich et al. 2011). It has been hypothesised that granules are a by-product of neuronal phagocytosis carried out by astrocytes or that they can be produced by astrocytes (Kuo et al. 1996). It has been recently proposed that aged neurons with impairments in their proteosomal/lysosomal degradation system form, as a protective strategy, 'budding-like' extrusions with accumulation of damaged or misfolded proteins and that subsequently, the aggregated extruded fibrillary material is engulfed by glia (Doehner et al. 2012).

In spite of all these studies, the results obtained until now are not yet conclusive and sometimes are contradictory. In this sense, it must be taken into account that staining of granules with polyclonal antibodies was found to be non-specific (Jucker et al. 1992). Our group recently reported that false positive stainings are due to the recognition of a neo-epitope in the granules by antibodies of IgM nature that are frequently present as a contaminant on commercial antibodies obtained from ascites or sera (Manich et al. 2014). The IgM and the

neo-epitope are responsible for numerous false positives, and the erroneous alleged presence of some components has distorted the study of these hippocampal granules. In any case, the significance of the neo-epitope and its possible role is unknown, and its location and appearance during the first phases of granule formation has not been explored yet.

The present work has been mainly focused on the observation under electron microscope of the hippocampal granules in the first stages of formation, in order to describe the granule formation process and to clarify their cellular origin. Moreover, we studied the presence of the neo-epitope during the granule formation process and its precise location in the mature and immature granules. The ultrastructural studies have been complemented by immunofluorescence studies.

Materials and methods

Mice

Aged male SAMP8 mice (9 or 14 months old) were used. They were kept at standard temperature conditions (22±2 °C) and 12:12-h light-dark cycles (300 lux/0 lux). Throughout the study, they had access to food and water ad libitum. All experimental procedures were reviewed and approved by the Ethical Committee for Animal Experimentation of the University of Barcelona (DAAM 6459).

Brain processing for ultrastructural observation on transmission electron microscopy and immunostaining with etched samples

The animals were anaesthetised intraperitoneally with 80 mg/kg of sodium pentobarbital and perfused intracardially with 50 mL of saline solution followed by 50 mL of p-formaldehyde (PF, Sigma-Aldrich) at 2 % in phosphate-buffered saline (PBS, pH 7.4). Coronal brain sections of 100-μm thickness were obtained with a vibratome. Sections were post-fixed with 2 % glutaraldehyde (Sigma-Aldrich) in PBS. The samples were treated with 1 % osmium tetraoxide (OsO_4) containing potassium ferricyanide for 1 h at 4 °C, dehydrated in acetone at 4 °C and finally embedded in Spurr resin. Semi-thin sections (1-μm thickness) were obtained, and after methylene blue staining, hippocampal CA1 regions were localised. Ultrathin sections (55-nm thickness) were obtained using a Reichert-Jung Ultracut E ultramicrotome and a diamond knife (Diatome, Switzerland), and the sections were then placed on gold grids and post-stained with uranyl acetate and lead citrate. Ultrathin sections were examined using a JEM-1010 transmission electron microscope operated at an accelerating voltage of 80 kV. The images were obtained using a Bioscan 792 camera (Gatan, CA, USA).

The grids used for immunostaining were previously etched with 5 % H_2O_2 for 6 min, washed for 5 min with distilled water (five times) and washed again with 0.1 M PBS for 5 min. Samples were then blocked for 30 min on drops of 1 % bovine serum albumin (BSA) in PBS and 20 mM glycine (Sigma-Aldrich) for 20 min, and incubated in the mouse IgM anti-neo-epitope primary antibody contained in anti-tau IgG antibody produced in mouse ascites (1/100, Merck Millipore, Darmstadt, Germany, see ref. Manich et al. 2014) in blocking buffer for 2 h. Then, the grids were washed four times with PBS, and sections were incubated for 1 h using an anti-mouse IgG secondary antibody coupled to 15-nm diameter colloidal gold particles (Jackson ImmunoResearch, Suffolk, UK) using a 1:30 dilution in blocking buffer. The incubation was followed by three washes with drops of PBS for 5 min, four washes with distilled water and air-drying. Controls of staining were performed omitting the primary antibody. Sections were stained with 2 % uranyl acetate in methanol and lead citrate.

Brain processing, freeze-substitution and immunostaining for transmission electron microscopy

For freeze-substitution, samples were chemically fixed by perfusion at 4 °C with a mixture of 4 % PF and 0.1 % glutaraldehyde in 0.1 M phosphate buffer (PB, pH 7.4). After washing with the same buffer containing 0.15 M glycine, samples were gradually infused in 30 % glycerol in the same buffer, as a cryoprotection, and then they were frozen in liquid propane at −188 °C (Leica EM CPC, Leica Microsystems, Vienna) and stored in liquid nitrogen at −196 °C until the freeze-substitution was done. Freeze-substitution was performed in an Automatic Freeze substitution System (AFS; Leica Microsystems), using methanol containing 0.5 % of uranyl acetate, for 3 days at −90 °C. On the fourth day, the temperature was slowly increased, by 5 °C/h, to −50 °C. At this temperature, samples were rinsed in methanol and then infiltrated and embedded in Lowicryl HM20 for 10 days. Ultrathin sections were obtained using a Leica Ultracut UC6

ultramicrotome (Leica Microsystems) and were picked up on Formvar-coated gold grids.

For the process of immunolabelling, sections were incubated at room temperature on drops of 5 % BSA in PBS for 20 min, followed by primary antibody chicken anti-GFAP IgG (1/50, Merck Millipore) or the mouse IgM anti-neo-epitope primary antibody contained in anti-tau IgG antibody produced in mouse ascites (1/100, Merck Millipore) in 1 % BSA in PBS for 2 h. After three washes with drops of 0.25 % Tween 20 in PBS for 30 min, sections were incubated for 1 h using a secondary antibody anti-chicken IgG or anti-mouse IgM coupled to 12- or 18-nm diameter colloidal gold particles (Jackson ImmunoResearch Laboratories) using a 1:30 dilution in 1 % BSA in PBS. This was followed by three washes with drops of PBS for 5 min, two washes with distilled water and air-drying. As a control for non-specific binding of the colloidal gold-conjugated antibody, the primary polyclonal antibody was omitted. Sections were stained with 2 % uranyl acetate in methanol and lead citrate and observed in a JEM-1010 electron microscope (Jeol, Japan) working at 80 kV, and the images were digitised with a Megaview III CCD camera.

Brain processing and immunohistochemistry for fluorescence and confocal microscopy

On one set of experiments, SAMP8 animals were anaesthetised intraperitoneally with sodium pentobarbital (80 mg/kg). They received an intracardiac gravity-dependent perfusion of 50 mL of saline solution. Brains were dissected and frozen by immersion in isopentane chilled in dry ice. Then, frozen brains were cut into 20-μm-thick sections on a cryostat (Leica Microsystems, Germany) at −22 °C and placed on slides. Sections were fixed with acetone for 10 min at 4 °C and frozen at −20 °C. On these sections, the immunohistochemistry procedures were performed as described in Manich et al. (2014). Briefly, sections were rehydrated with PBS and they were blocked and permeabilised with 1 % BSA (Sigma-Aldrich, Madrid, Spain) and 0.1 % Triton-X-100 (Sigma-Aldrich) in PBS for 20 min. Sections were then washed with PBS and incubated overnight with both the chicken primary antibody anti-GFAP IgG (1/300, Merck Millipore) and the mouse IgM anti-neo-epitope primary antibody contained in anti-tau IgG antibody produced in mouse ascites (1/100, Merck Millipore, see ref. Manich et al. 2014). Slides were washed and incubated for 1 h at room temperature with the secondary antibodies AlexaFluor 488 goat anti-chicken IgG (1/250, Life Technologies, Carlsbad, CA) and goat anti-mouse IgM-TRITC (1/50, Jackson Immunoresearch Laboratories). Nuclear staining was done with Hoechst (H-33258, Fluka, Madrid, Spain), and slides were washed and coverslipped with Prolong Gold antifade reagent (Life Technologies). Controls of staining were performed incubating only with PBS, or with PBS and the secondary antibodies. Antibody cross-reactivity controls were also performed. Images of all the hippocampal clusters and GFAP-positive astrocytes contained in three brain sections of four 9-month-old SAMP8 mouse were taken using a fluorescence laser microscope (BX41, Olympus, Germany) and stored in tif format. These images were obtained in green, red and ultraviolet channels using a×20 objective. Random selected GFAP-positive astrocytes and clusters of granules were also obtained with the×60 objective. For each magnification, all images were acquired using the same laser and software settings. Images of selected areas that contain clusters of granules that colocalise with a GFAP reactive astrocyte were also taken with confocal scanning laser microscope (TCS/SP2, Leica Microsystems) for fine colocalisation analysis. Orthogonal sections were obtained from these images to analyse the colocalisation and spatial distribution of the fluorescence staining.

On another set of experiments, SAMP8 animals were perfused intracardially with 50 mL of saline solution followed by 50 mL of PF (Sigma-Aldrich) at 4 % in PBS. Brains were then dissected, post-fixed 4 h in PF at 2 % in PBS and cryoprotected by immersion in PBS with 30 % sucrose for 24 h. Afterwards, brains were frozen by immersion in isopentane chilled in dry ice and stored at −80 °C until further use. Then, frozen brains were cut into 20-μm-thick sections on a cryostat (Leica Microsystems, Germany) at −22 °C and placed on slides. Using the same immunohistochemistry procedures described before, a double staining of some sections with rat anti-CD11b directed against microglia (1/100, Merck Millipore) and the goat anti-Syndecan antibody (1/100, Santa Cruz Biotechnology, CA) has been performed. This antibody has been proved to contain IgM antibodies directed against the neo-epitope. Secondary antibodies were AlexaFluor 488 donkey anti-rat IgG

(1/250, Life Technologies, Carlsbad, CA) and AlexaFluor 555 donkey anti-goat IgG (1/250, Jackson Immunoresearch Laboratories). This last secondary antibody has cross-reactivity with the IgM. Other sections have been double stained with mouse anti-CNP directed against oligodendrocytes (1/100, Abcam, UK) and the goat anti-Syndecan (1/100, Santa Cruz Biotechnology, CA) to stain the neo-epitope. In this case, secondary antibodies were AlexaFluor 488 donkey anti-rat IgG (1/250, Life Technologies, Carlsbad, CA) and AlexaFluor 555 donkey anti-goat IgG (1/250, Jackson Immunoresearch Laboratories) in the second one. Sections were observed, and some images were taken using the same fluorescence laser microscope (BX41, Olympus, Germany).

Astrocyte and cluster diameter quantification

The diameters of the GFAP-positive astrocytes and those of the granule clusters were measured using the Image J program (National Institute of Health, USA) on images obtained with the×20 objective. In both cases, each region of interest (ROI) was selected by using the "freehand selection" tool of the Image J program, manually tracing the contour of the area of influence of each astrocyte or granule cluster, as exemplified in the ROIs indicated in Fig. 5a. For each ROI, the Feret's diameter (the longest distance between any two points along the selection boundary, also known as maximum calliper) was determined. As the fine extreme processes of the astrocytes are not visible at×20 magnification, Feret's diameter values of the astrocytes have been corrected by the factor 1.23. This factor was calculated after comparing the value obtained for some astrocytes in both the×60 and the×20 magnification. The measure of the Feret's diameter of the granule clusters was not affected by the magnification, and thus, it has not been corrected.

Statistical analysis

Statistical analyses were performed by means of ANOVA, *t* test for dependent samples and correlation analysis by using Statistica for Windows (Stat Soft Inc.). Differences were considered statistically significant when $p<0.05$.

Results

Ultrastructural characterisation of mature hippocampal granules

A portion of the hippocampal neuropil from SAMP8 mice aged 14 months is shown in Fig. 1. In this area, several mature and immature granules from the same cluster can be visualised. Mature granules measured up to 3 μm in diameter and presented a core formed by a dense mesh of electron-dense membranous-like structures when tissues were embedded in Spurr and treated with OsO_4. This core was surrounded by an electron-translucent region (halo), and this halo was encircled by a plasma membrane (Fig. 2a). On the other hand, granules appeared practically translucent in sections embedded in Lowicryl, without OsO_4 (Fig. 2b). As OsO_4 highlights the lipidic compounds, this observation indicates a high lipidic content of the granules core. On Spurr-embedded tissues, the translucent region contained some blebs or big cisterns, which seemed to originate from invaginations of the surrounding plasma membrane, but could also be near or maintain a close contact with the core of the granules (Fig. 2a, c). Small granular structures compatible with glycogen and some cellular organelles, like mitochondria (Fig. 2a, d), usually in a degenerating state (Fig. 2d) are also observed in the translucent region. Moreover, the plasmatic membrane surrounding the granules frequently showed some characteristic junction with the membranes of adjacent cells (Fig. 2a, b), described by Kuo et al. (1996) as astrocyte-astrocyte junctions. These junctions between astrocytes were also observed in some hydropic astrocyte end-feets around the blood vessels, an area where some granules have also been visualised (data not shown).

In general, the structures contained in the immediately surrounding area of the mature granules do not present perceivable morphological alterations. Occasionally, some symptoms of worsening have been detected, such as degenerating dendrites (Fig. 2a) or presynaptic buttons with mitochondria suffering a mitophagic process (Fig. 2d). Other pathologic signs present in the hippocampal tissue but not always close to the granules were hydropic astrocytes with signs of swelling (data not shown).

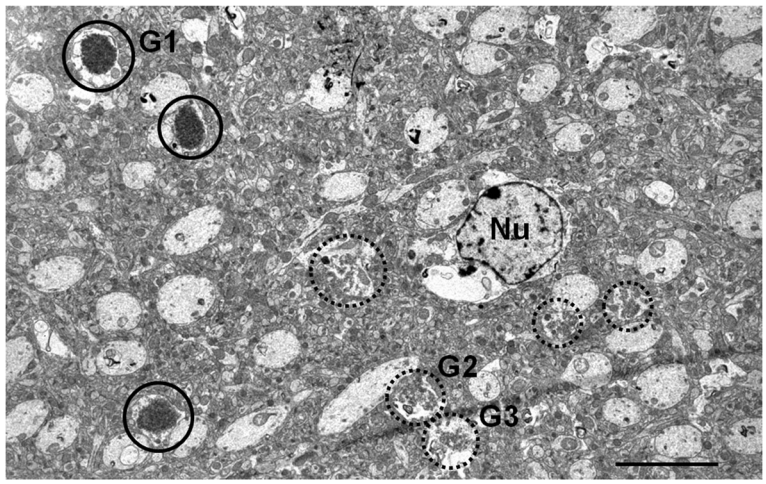

Fig. 1 Electron microscopy image of a hippocampal CA1 region from a 14-month-old SAMP8 mouse in which some mature (*circle*) and immature (*dashed circle*) granules can be observed. *Nu* astrocyte nucleus, *G1* magnification illustrated in Fig. 2a, *G2* and *G3* magnification illustrated in Fig. 3a. *Scale bar* 5 μm

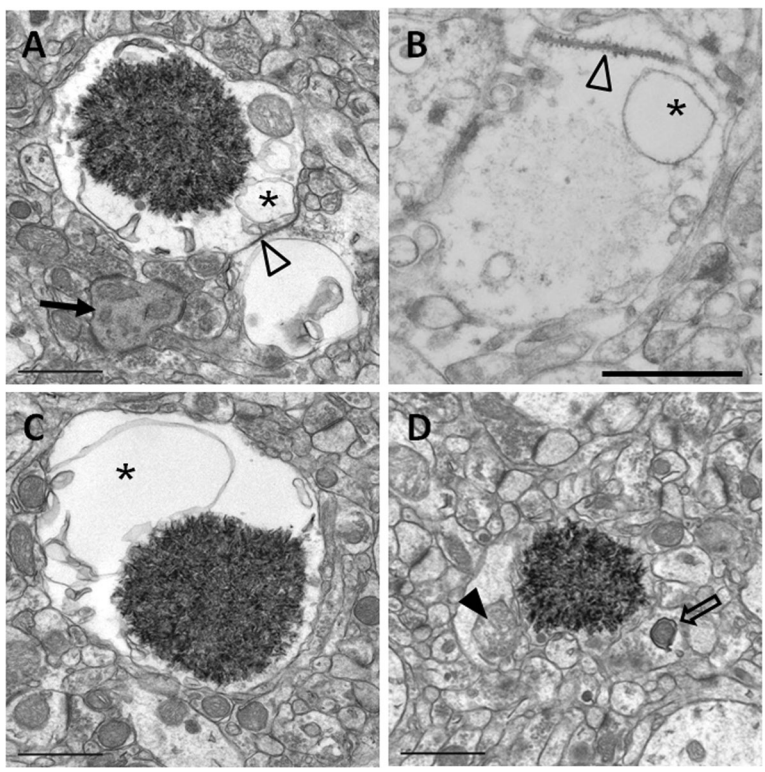

Fig. 2 Electron microscopy images of hippocampal mature granules from 14-month-old SAMP8 mice. Mature granules measured up to 3 μm. When tissue was embedded in Spurr and treated with OsO_4, granules showed an electron-dense core formed by a dense mesh of fibrillar membranous-like structures, generally encircled by a translucent halo (**a**, **c**, **d**). When tissue was embedded in Lowicryl, the core appeared smoothly stained (**b**). Blebs or big cisterns (*asterisks*), as well as degenerating mitochondria (*full arrowhead*), are located in the translucent area. A characteristic junction with a membrane of an adjacent cell can be observed (*empty arrowhead*). In the surroundings of the mature granule, a degenerating dendrite (*full arrow*) and a mitophagy process (*empty arrows*) can be visualised. *Scale bar* 1 μm

Ultrastructural characterisation of immature hippocampal granules

As SAMP8 animals show a progressive and sustained increase of the number of granules and clusters, at the studied ages, it was expected to find not only already formed granules but also granules in process of formation. Occasionally, granules that presented some sparse membranous-like structures, instead of a compact core, have been observed. We judged these structures, not described formerly, as granules in the first stages of their formation (immature granules). In Fig. 1, some immature granules close to the mature granules could be observed. In Fig. 3, several immature granules from 14-month-old mice are shown at high magnification. There are some features that are repeated in almost all the immature granules. The most characteristic is the presence, in the translucent zone, of membranous structures that form intracellular bubbles or blebs, of variable sizes and irregular shapes, generally not spherical (Fig. 3a, b). Although in some cases they resemble the smooth endoplasmic reticulum, blebs are generally not equivalent to any of the membranous organelles. Some of the blebs appeared merged with the plasma membrane, while others reached the membranous matrix of the inside of the granule (Fig. 3a, b). In some cases, bleb membranes close to the core seem to fragment, and membrane fragments appear to be incorporated to the matrix (Fig. 3b). Degenerating mitochondria could also be observed in the translucent zone (Fig. 3a, b), and in some cases, waste parts of the mitochondrial membrane seemed to be projected towards the central zone of the granule in formation (Fig. 3b). The plasma membrane of the immature granules is often fragmented or unstable, as well as some membranes of adjacent structures, thus loosing the boundaries between the cell where the granule is formed and the adjacent structures (Fig. 3a–c, and a magnified region from Fig. 3a shown in Fig. 3d). These phenomena of membranous rupture of cellular structures adjacent to the immature granules are particularly evident in granules in formation and causes that part of the neuropil next to the granule will be incorporated to it. For instance, in Fig. 3c, a presynaptic button with its vesicles could be observed, without part of the external membrane, and thus connected to the translucent area of the adjacent granule.

On the other hand, some ultrathin sections were immunostained with anti-GFAP antibodies, and glial filaments positively labelled could be occasionally observed on the translucent region of some granules, near the forming core of the immature granules (Fig. 3e). Moreover, some immature granules have been observed in some hydropic end-feet processes of the astrocytes surrounding the blood vessels, in which some astrocytic junctions as those described above were present (data not shown).

Fine localisation of the neo-epitope on the granules

The immunostaining with the IgM antibody directed against the neo-epitope in Lowicryl-embedded sections allowed the determination of the precise location of the neo-epitope on the granules (Fig. 4a). The nanogold particles intensely stained the granules and were mainly located in the core, although few of them could be observed next to the plasma membrane or in adjacent structures (Fig. 4b). In the sections embedded in Spurr, it could be observed that the nanogold particles contained in the core are specifically located on the fragments of the membranous structures (Fig. 4c, d). In the translucent zone, the staining was only located in membranous remnants (similar to those present in the core) but absent in the cytoplasm. In the immature granules (Fig. 4e, f), the staining was located mainly in the region where the core is forming, but it could also be distinguished in some membranes of the adjacent structures.

Relationship between the clustered granules and the astrocytic cells

Simultaneous fluorescence immunostaining with IgM antibodies directed against the neo-epitope and anti-GFAP antibodies allowed the visualisation of the clustered hippocampal granules of SAMP8 mice as well as GFAP-positive astrocytes. In most cases, there is no relationship between GFAP-positive astrocytes and clusters, but sometimes the region occupied by a certain GFAP-positive astrocyte coincided with that occupied by the cluster of granules (Fig. 5a). In those cases, the observation of both structures using confocal microscopy confirmed a close relationship between the astrocytic processes and the granules, i.e. the granules were located next to astrocytic processes without exception (Fig. 5b), and some granules were even surrounded by the processes (Fig. 5c). Simultaneous fluorescence immunostaining has also been performed with (a) IgM antibodies and anti-CD11 antibodies, a marker for microglial cells, and (b) IgM antibodies and anti-CNP antibodies, directed against oligodendrocytes. In any of these cases, the positive cells have been observed to be related neither to the granules nor to the clusters

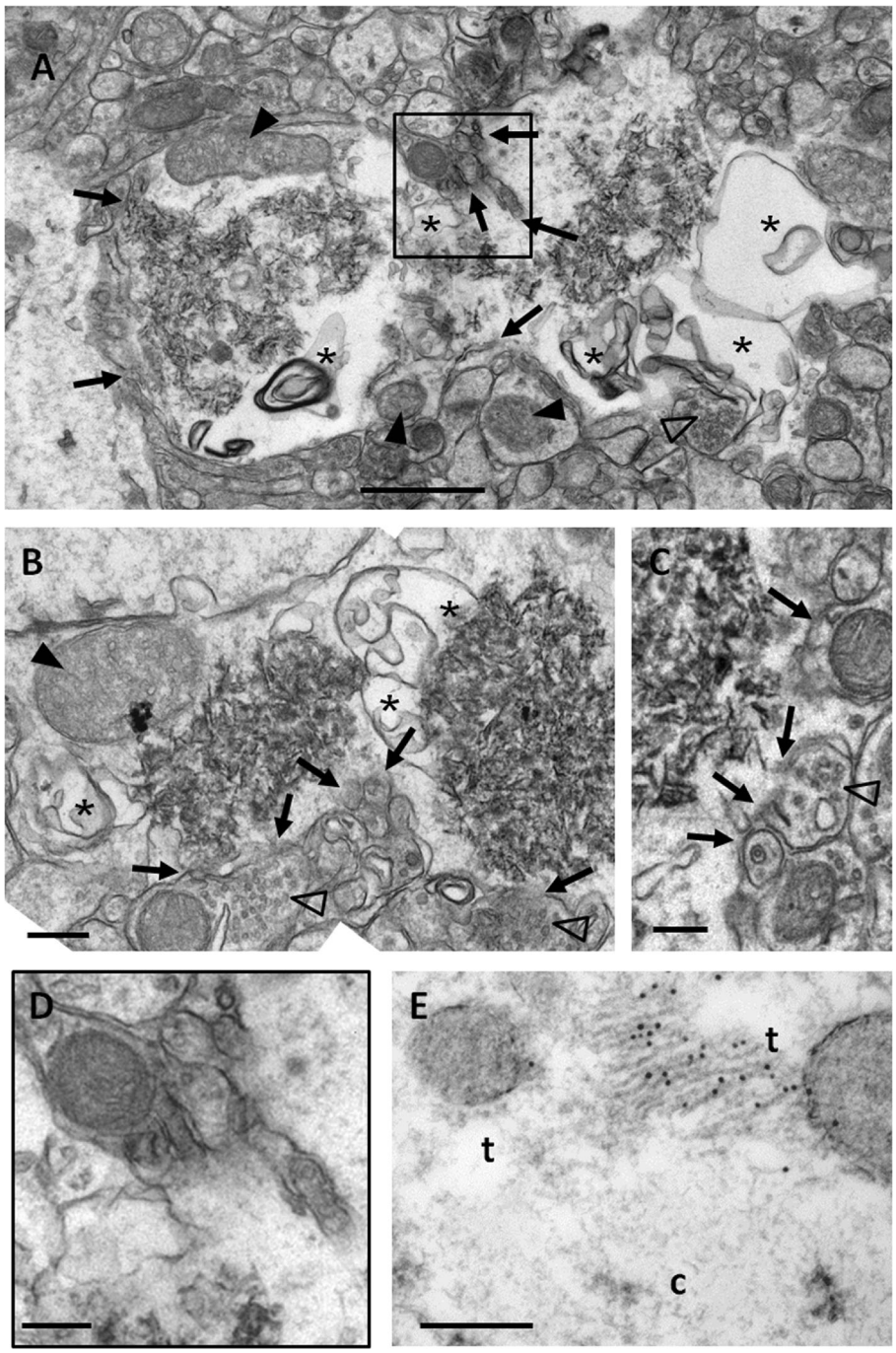

Fig. 3 Electron microscopy images of hippocampal immature granules from 14-month-old SAMP8 mice. **a** Immature granules showed, instead of the electron-dense core, some sparse membranous-like structures. **b**, **c** Granules in a more advanced stage of development. Big blebs or bubbles (*asterisk*s) and degenerating mitochondria (*full arrowheads*) appeared in the peripheral zone. The plasma membrane and membranes of adjacent structures showed instability and fragmentation (*full arrows*), causing a loose of the boundaries of these structures. This process of rupture can affect dendritic spines (*empty arrowheads*), as clearly shown in **c.** **d** Inset from **a** in which the instability and the fragmentation of the membranes could be better observed. **e** Immunoelectron GFAP staining in Lowicryl-embedded tissue. GFAP-positive fibrils labelled with nanogold particles appeared on the translucent area (*t*), near to the forming core (*c*) of an immature granule. *Scale bar* in **a**, **b** 1 μm. *Scale bar* in **c**–**e** 200 nm

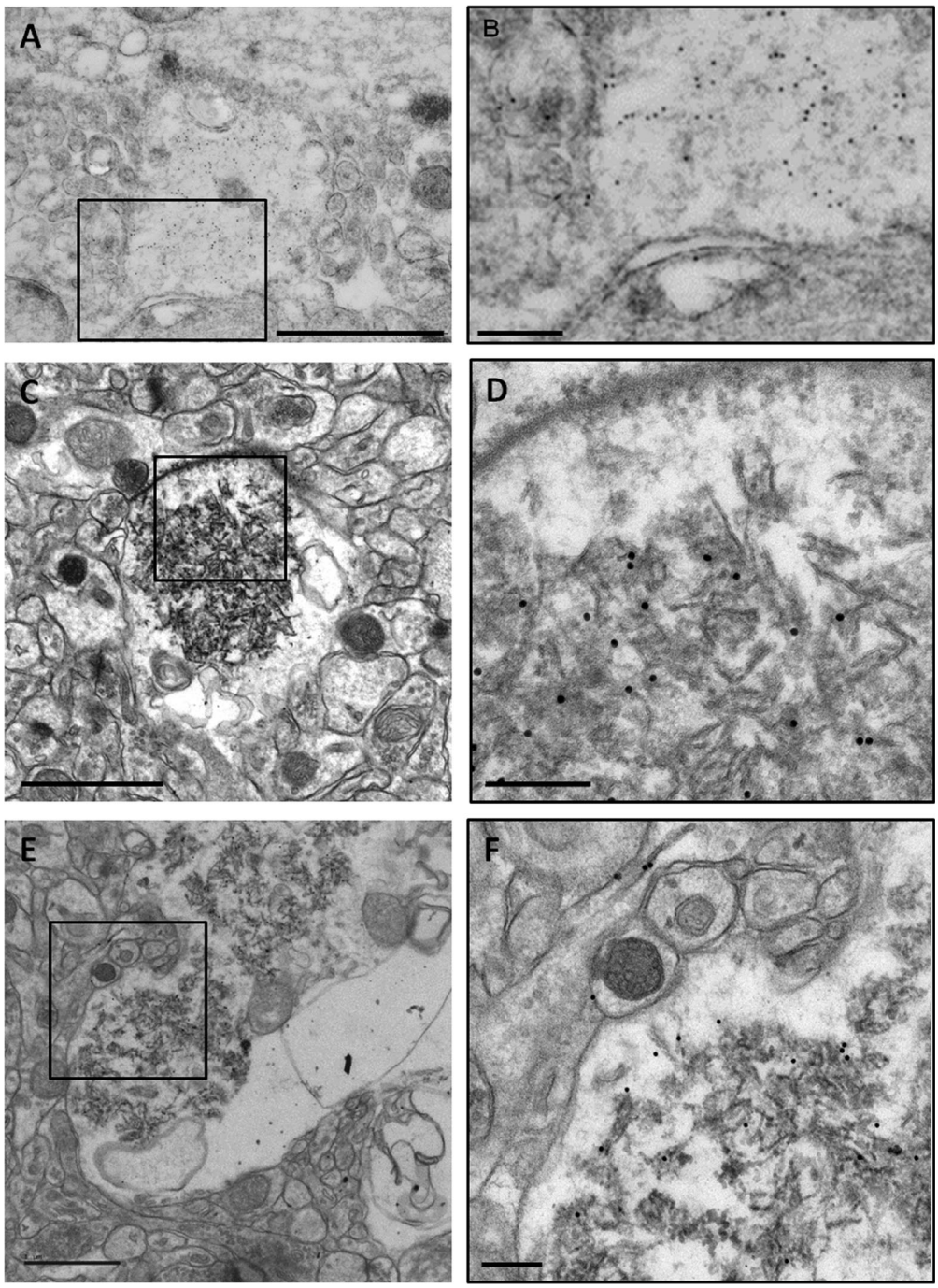

Fig. 4 Immunoelectron microscopy images of hippocampal granules of 14-month-old SAMP8 mice stained with IgM antibodies directed against the neo-epitope. **a** A granule of an ultrathin section embedded in Lowicryl is shown. The staining of the antibody is abundantly located in the core of the granule. **b** Inset of **a. c** An ultrathin section embedded in Spurr that presents a mature granule stained with the IgM anti-neo-epitope antibody. **d** Inset of **c**, in which the nanogold particles were observed located in the fibrils constituting the core of the granule but not in the halo. **e** Immature granules stained with the IgM anti-neo-epitope antibody. **f** Inset of **e**, in which the staining of the antibody appeared located in the sparse fibrils of the core in process of formation but not in the translucent area. Some membranes on adjacent structures occasionally presented staining. *Scale bar* in **a**, **c**, **e** 1 μm. *Scale bar* in **b**, **d**, **f** 200 nm

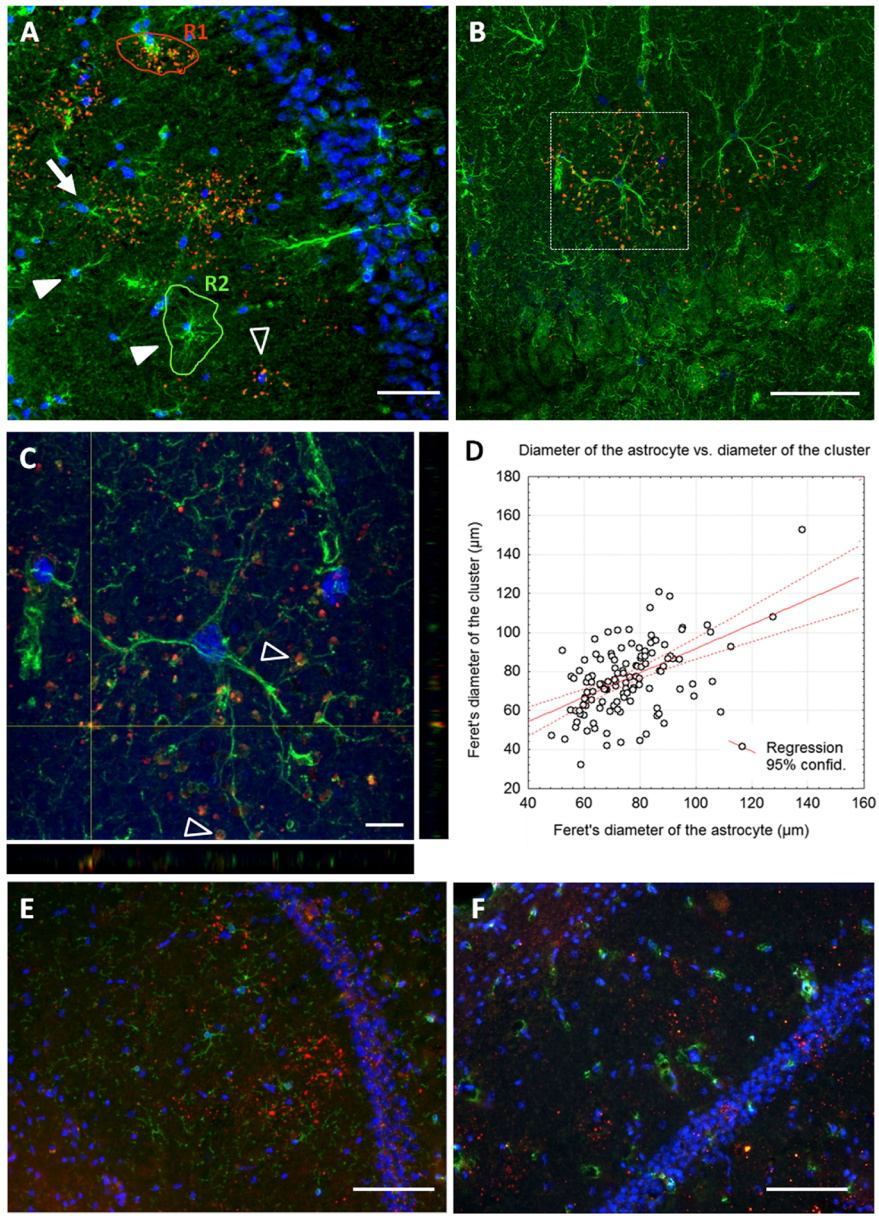

Fig. 5 **a**–**c** Double immunohistochemical staining of the CA1 hippocampus area from 9-month-old SAMP8 mice. The granules were detected with the mouse IgM antibody against the neo-epitope (*red*), and the reactive astrocytes were detected with an anti-GFAP antibody (*green*). Nuclei were stained by Hoechst (*blue*). **a** Fluorescence microscopy allowed the observation of some clusters in the CA1 region, which were found alone (*empty arrowheads*) or associated with an astrocyte (*arrow*). Some astrocytes did not present any associated cluster (*full arrowheads*). *R1* and *R2* exemplify a ROI for a granule cluster and a ROI for an astrocyte, respectively (see "Materials and methods" section). **b** Image from confocal microscopy showed the close association of some clusters to the astrocytes. **c** Inset of B in which two orthogonal projections are shown. The granules were found close to the astrocyte processes and even encircled by them (*empty arrowheads*). **d** Correlation graph between the Feret's diameter of the clusters and that of the GFAP-positive astrocytes from data obtained from clusters and GFAP-positive astrocytes that colocalised. **e** Double immunohistochemical staining with rat *anti-CD11b directed against microglia (green)* and IgM anti-neo epitope (red). Nuclei were stained by Hoechst (blue). F) Double immunohistochemical staining with mouse anti-CNP directed against oligodendrocytes (*green*) and IgM anti-neo epitope (*red*). Nuclei were also stained by Hoechst (*blue*). In any of these cases, the positive cells (microglia or oligodendrocytes) have been observed to be related neither to the granules nor to the clusters. *Scale bar* in **a**, **e**, **f** 100 µm; **b** 50 µm; **c** 10 µm (colour figure online)

(Fig. 5e, f). Thus, astrocytes, but not microglia or oligodendrocytes, are candidate to be related to the pathological process related to the granule formation.

As it is indicated, only some granule clusters match with the area of influence of a GFAP-positive astrocyte. However, the size of the clusters appears to be somehow constant and similar to that of GFAP-positive astrocytes. To compare the sizes of both structures, a morphometric study was performed by determining the Feret's diameter of clusters and that of GFAP-positive astrocytes present in different sections from the hippocampus of SAMP8 mice. The Feret's diameter from 450 clusters and 610 astrocytes has been measured. In 123 cases, the cluster colocalised with a GFAP-positive astrocyte. However, the remaining 487 GFAP-positive astrocytes were not related with a granule cluster and the other 327 granule clusters did not show any relation with a GFAP-positive astrocyte. The mean Feret's diameter of astrocytes was 71.289 μm (±0.562 μm), whereas the mean Feret's diameter of the clusters was 72.984 μm (±0.853 μm). The ANOVA analysis did not indicate significant differences between them, being $F_{(1,1058)}=2.98$ and $p>0.05$. On the other hand, the relationship between the two variables was studied considering the 123 cases where the astrocytes and the clusters colocalised. The Student's t test for paired data resulted in not statistically significant differences between the Feret's diameter of the astrocytes and that of the clusters, being $t_{122}=0.556$ and $p>0.5$. The correlation studies between both variables showed a $R=0.5045$ and a $p<0.001$, thus indicating a positive correlation between the diameter of the astrocyte and that of the associated cluster (Fig. 5d).

Discussion

In this study, we describe the formation process of the pathological granules that appear in the hippocampus of aged mice and provide new data about their cellular origin. To our knowledge, this is the first study which shows the ultrastructure of the immature granules and their formation process. In addition, we also determine that the neoepitope recently described in the mature granules emerges in the first stages of the granule formation.

Results obtained in the present study indicated that mature granules were located in the astrocytic processes. Although the translucent zone of the granules was formed by disturbed cytoplasm, and it was then difficult to identify the cell where the granule was located, immunohistochemical studies on ultrathin sections revealed in some cases the presence of GFAP fibrils in this zone. Moreover, small granular structures resembling glycogen accumulations, which are characteristic of astrocytes, were also found in the translucent zone. Furthermore, we also observed that the plasma membrane of various granules showed junctions with the membrane of some adjacent cells, which seems characteristic of the junctions between astrocytes (Kuo et al. 1996) and are similar to gap junction channels described in Nagy et al. (1999). We would like to point out that no synaptic vesicles or presynaptic buttons have been observed in the mature granules, neither in the core nor in the translucent zone. The relationship between granules and astrocytes is also shown in some cases in which the granules are located in astrocyte end-feets surrounding blood capillaries. Thus, these results agree with those of Jucker et al. (1994) and Kuo et al. (1996), which suggested the astrocytes as the cells where the granules are originated.

The results of this study also suggested that there was an unambiguous relationship between the granule clusters and the astrocytes. As it has been previously described (Jucker et al. 1992; Manich et al. 2011), the double immunofluorescence staining with antibodies against GFAP protein and antibodies that stained granules showed in some cases that the granule cluster is distributed in correspondence with the reactive astrocyte. This relationship has not been observed with other cellular types, like oligodendrocytes or microglia. These cases of colocalisation of the cluster and the GFAP-positive astrocyte represent, however, a small percentage in the present study performed with 9-month-old SAMP8 mice: only the 20.16 % of GFAP-positive astrocytes showed an association with a cluster, and only the 27.33 % of the clusters are associated with a GFAP-positive astrocyte. We believe therefore that there is not a causal relationship between the reactivity for GFAP and the presence of clusters; but the fact that clusters and GFAP-positive astrocytes occupied spherical regions of similar sizes according to Feret's diameters, reinforce the idea that each cluster is probably uniquely associated with a particular astrocyte, whether this astrocyte is GFAP-reactive or not. In some cases, this astrocyte is GFAP-positive whereas in some other cases, it would be a non-reactive astrocyte or an astrocyte which has lost this reactivity due to the degenerative processes that seem to accompany the formation of the granules. In addition, as it has been shown in the "Results" section,

when an immature granule is visualised using ultrastructural studies, it is likely to find other immature granules in the nearby areas of the neuropil and in some cases, even in the area of the same astrocytic process. This suggests that in different regions of the same astrocyte, there is a generation of granules that will give rise to the cluster.

According to the pattern already described (Del Valle et al. 2010), the clustered granules mainly start their formation in the CA1 region of the hippocampus, and then they expand gradually to regions CA2 and CA3. It is frequent to find granule clusters close to each other. Thus, a possible explanation of the expansion of the clusters in the hippocampal astrocytes could be the communication network between astrocytes through the gap junction channels, formed by connexins 30 and 43, and constituting the glial syncitium (Giaume et al. 2010). Gap junction channels are observed at the interface of the neighbouring astrocytes and in the contacts between the astrocytes end-feets surrounding blood vessels. In the present study, the junctions observed next to the granules in the ultrathin sections resembled those observed in the hydropic astrocyte end-feets which surround brain blood vessels. In addition, some granules have also been found in these end-feets. Moreover, in pathological situations, the expression of connexins is upregulated, especially when the astrocytes are close to some lesions (Ochalski et al. 1995; Theriault et al. 1997).

The astrocytes of the CA1 region are also characterised for being more sensitive to oxidative stress in comparison to other areas of the hippocampus, as reported in transitory focal ischaemia (Ouyang et al. 2007), as well as for their higher coupling compared to the CA3, as shown in dye coupling studies (D'Ambrosio et al. 1998). These facts might explain the clustered granules' appearance in the CA1 zone at the beginning of their formation. Moreover, the SAMP8 mice are a known model of oxidative stress because of the high levels presented at early ages (Alvarez-García et al. 2006; Pallàs et al. 2013). Thus, the high levels of oxidative stress could explain the early appearance of the granules in the CA1 zone of the hippocampus in comparison to other mouse strains. Furthermore, a diminishment of the granule expression was observed after dietary ingestion of antioxidant compounds, such as resveratrol in SAMP8 mice (Porquet et al. 2013) or an antioxidant diet in ApoE-deficient mice (Veurink et al. 2003).

Another important aspect of this work is the study of the granule formation process. The results suggested that in the affected astrocytes processes, some of them clearly swollen or hydropic astrocytes, there is a process of vacuolisation or digestion of the cytoplasmic components and intracellular organelles that results in the formation of waste or debris. This waste includes membranous fragments, which generate a spread matrix of fibrils and thereafter the dense-core of the granule. In the regions where the granules are forming the plasma membrane of astrocytes appears to show some instability revealed by a certain degree of fragmentation, a less electron-dense appearance than the outermost regions, and the presence of irregular invaginations and evaginations of variable sizes. In these unstable regions, some effects, which can be really aggressive, can also be observed on adjacent structures. In some cases, there are regions of neuropil where the cellular elements, including the presynaptic buttons and the dendritic spines with their secretory vesicles, appeared disrupted and are incorporated into the astrocytic region. The incorporation of the secretory vesicles may lead to the false interpretation that the granule is located in a neuronal component, as suggested by Mitsuno et al. (1999). Our results seem to indicate that glia do not engulf aggregated material, as postulated by Doehner et al. (2012), but the aggregation of the material is produced inside the astrocyte from its own material and material coming from nearby neuropil regions.

It remains to be elucidated why once the granules are formed the region seems to stabilise, and only some symptoms of worsening are observed, like a degenerating dendrite or a presynaptic button with a mitochondria suffering a mitophagy process. However, these observations show that granules are the manifestation of an astrocytic degenerative process that could produce a neurodegenerative disease and should not be understood as a mere accumulation of waste substances. It is conceivable that the presence of the granules produces some functional alterations, and this could be especially noteworthy in old SAMP8 animals, in which clusters occupy almost the entire hippocampus.

From this point of view, the study from Soontornniyomkij et al. (2012) performed with the C57BL/6 N strain with animals up to 26 months of age showed interesting results. They indicated that there was a negative correlation between the number of granule clusters and the discrimination ratio obtained by the object recognition test. Although the interpretation

made should be reviewed due to the probable presence of contaminant IgM antibodies directed against the neo-epitope, the fact that increased granule clusters are negatively correlated with the ability of discrimination of objects reinforces the idea that the presence of granules is probably related to functional alterations.

Regarding the neo-epitope present in the granules, it could be observed that their presence is very high in the core of mature granules and in the region where the core is forming in immature granules. In both cases, the neo-epitope appeared associated with membranous fragments that will be located in the core of the granules. This fact suggested that the neo-epitope is produced during the formation of these fragments, although a certain labelling was occasionally observed in the membranes of adjacent structures. The neo-epitope, therefore, does not seem to be a trigger or a key element in the formation of granules, but its presence could be related to a possible immune response to the disease process that is occurring.

In conclusion, the present study shows that the granules formed with age in the hippocampus of mice are the result of a degenerative disease process that occurs primarily in astrocytes although nearby neuronal structures may also be affected. The formation of a granule in a particular astrocyte is not a punctual fact, but the different fingerings of the same astrocyte will host different granules resulting in the formation of a granule cluster. During the granule formation, different membranous fragments are generated and they will form part of the core of the granule. Moreover, the neo-epitope will be generated during the formation of these fragments. Further investigations are required to determine the cause of the granule formation and to establish the function of the neo-epitope.

Acknowledgments This study was funded by grants BFU2010-22149, SAF2011-23631 and SAF2012-39852 from Spain's Ministerio de Ciencia e Innovación, and Centros de Investigación Biomédica en Red (CIBER) from Instituto de Salud Carlos III. We would like to thank Generalitat de Catalunya for funding the research group (2009/SGR00853) and for awarding a predoctoral fellowship to G. Manich (FI-DGR 2011). P.P. Liberski was supported with a HARC EC grant. We are thankful to Dr. Núria Cortadellas and Dr. Carmen López from the Servei de Microscòpia Electrònica and Dr. Anna Bosch from the Servei de Microscòpia Confocal (Centres Científics i Tecnològics, Universitat de Barcelona), for their help with the microscopy services. We are also grateful to Dr. Albert Martínez and Dr. Carme Auladell for their advice about transmission electron microscopy studies.

References

Akiyama H, Kameyama M, Akiguchi I, Sugiyama H, Kawamata T, Fukuyama H, Kimura H, Matsushita M, Takeda T (1986) Periodic acid-Schiff (PAS)-positive, granular structures increase in the brain of senescence accelerated mouse (SAM). Acta Neuropathol 72:124–129

Alvarez-García O, Vega-Naredo I, Sierra V, Caballero B, Tomás-Zapico C, Camins A, García JJ, Pallàs M, Coto-Montes A (2006) Elevated oxidative stress in the brain of senescence-accelerated mice at 5 months of age. Biogerontology 7:43–52

D'Ambrosio R, Wenzel J, Schwartzkroin PA, McKhann GM, Janigro D (1998) Functional specialization and topographic segregation of hippocampal astrocytes. J Neurosci 18:4425–4438

Del Valle J, Duran-Vilaregut J, Manich G, Casadesús G, Smith MA, Camins A, Pallàs M, Pelegrí C, Vilaplana J (2010) Early amyloid accumulation in the hippocampus of SAMP8 mice. J Alzheimers Dis 19:1303–1315

Doehner J, Madhusudan A, Konietzko U, Fritschy JM, Knuesel I (2010) Co-localization of Reelin and proteolytic AβPP fragments in hippocampal plaques in aged wild-type mice. J Alzheimers Dis 19:1339–1357

Doehner J, Genoud C, Imhof C, Krstic D, Knuesel I (2012) Extrusion of misfolded and aggregated proteins—a protective strategy of aging neurons? Eur J Neurosci 35:1938–50

Giaume C, Koulakoff A, Roux L, Holcman D, Rouach N (2010) Astroglial networks: a step further in neuroglial and gliovascular interactions. Nat Rev Neurosci 11:87–99

Irino M, Akiguchi I, Takeda T (1994) Ultrastructural study of PAS-positive granular structures in brains of SAMP8. Takeda T. International Congress Series; The Sam Model Of Senescence. pp371-374

Jucker M, Walker L, Martin L, Kitt C, Kleinman H, Ingram DK, Price D (1992) Age-associated inclusions in normal and transgenic mouse brain. Science 255:1445

Jucker M, Walker LC, Schwarb P, Hengemihle J, Kuo H, Snow D, Bamert F, Ingram DK (1994) Age-related deposition of glia-associated fibrillar material in brains of C57BL/6 mice. Neuroscience 60:875–89

Knuesel I, Nyffeler M, Mormède C, Muhia M, Meyer U, Pietropaolo S, Yee BK, Pryce CR, LaFerla FM, Marighetto A, Feldon J (2009) Age-related accumulation of Reelin in amyloid-like deposits. Neurobiol Aging 30:697–716

Krass KL, Colinayo V, Ghazalpour A, Vinters HV, Lusis AJ, Drakec TA (2003) Genetic loci contributing to age-related hippocampal lesions in mice. Neurobiol Dis 13:102–108

Kuo H, Ingram DK, Walker LC, Tian M, Hengemihle JM, Jucker M (1996) Similarities in the age-related hippocampal deposition of periodic acid-schiff-positive granules in the senescence-accelerated mouse P8 and C57BL/6 mouse strains. Neuroscience 74:733–740

Lamar CH, Hinsman EJ, Henrikson CK (1976) Alterations in the hippocampus of aged mice. Acta Neuropathol 36:387–391

Manich G, Mercader C, Del Valle J, Duran-Vilaregut J, Camins A, Pallàs M, Vilaplana J, Pelegrí C (2011) Characterization of amyloid-β granules in the hippocampus of SAMP8 mice. J Alzheimers Dis 25:535–546

Manich G, del Valle J, Cabezón I, Camins A, Pallàs M, Pelegrí C, Vilaplana J (2014) Presence of a neo-epitope and absence of amyloid beta and tau protein in degenerative hippocampal granules of aged mice. AGE 36:151–65

Mitsuno S, Takahashi M, Gondo T, Hoshii Y, Hanai N, Ishihara T, Yamada M (1999) Immunohistochemical, conventional and immunoelectron microscopical characteristics of periodic acid-Schiff-positive granules in the mouse brain. Acta Neuropathol 98:31–38

Nagy JI, Patel D, Ochalski PA, Stelmack GL (1999) Connexin30 in rodent, cat and human brain: selective expression in gray matter astrocytes, co-localization with connexin43 at gap junctions and late developmental appearance. Neuroscience 88:447–68

Ochalski PA, Sawchuk MA, Hertzberg EL, Nagy JI (1995) Astrocytic gap junction removal, connexin43 redistribution, and epitope masking at excitatory amino acid lesion sites in rat brain. Glia 14:279–294

Ouyang YB, Volobouéva LA, Xu LJ, Giffard RG (2007) Selective dysfunction of hippocampal CA1 astrocytes contributes to delayed neuronal damage after transient forebrain ischemia. J Neurosci 27:4253–60

Pallàs M, Porquet D, Vicente A, Sanfeliu C (2013) Resveratrol: new avenues for a natural compound in neuroprotection. Curr Pharm Des 19:6726–31

Porquet D, Casadesús G, Bayod S, Vicente A, Canudas AM, Vilaplana J, Pelegrí C, Sanfeliu C, Camins A, Pallàs M, Del Valle J (2013) Dietary resveratrol prevents Alzheimer's markers and increases life span in SAMP8. AGE 35:1851–65

Robertson T, Dutton NS, Martins RN, Roses AD, Kakulas BA, Papadimitriou JM (1998) Age-related congophilic inclusions in the brains of apolipoprotein E-deficient mice. Neuroscience 82:171–180

Soontornniyomkij V, Risbrough VB, Young JW, Soontornniyomkij B, Jeste DV, Achim CL (2012) Increased hippocampal accumulation of autophagosomes predicts short-term recognition memory impairment in aged mice. AGE 34:305–316

Theriault E, Frankenstein UN, Hertzberg EL, Nagy JI (1997) Connexin43 and astrocytic gap junctions in the rat spinal cord after acute compression injury. J Comp Neurol 382:199–214

Veurink G, Liu D, Taddei K, Perry G, Smith MA, Robertson TA, Hone E, Groth DM, Atwood CS, Martins RN (2003) Reduction of inclusion body pathology in ApoE-deficient mice fed a combination of antioxidants. Free Radic Biol Med 34:1070–1077